Distortional Strength and DSM Design of Cold-Formed Steel Lipped Channel Beams under Transverse Loadings

Lucas Aguiar Pigliasco da Fonseca[1], Alexandre Landesmann[1], Dinar Camotim[2]

[1]*Programa de Engenharia Civil, PEC/COPPE/UFRJ, Universidade Federal do Rio de Janeiro*
Av. Athos da Silveira Ramos-149. Centro de Tecnologia – Bloco B, Sala 101, 21941-909, Rio de Janeiro, Brazil
lucaspigliasco@coc.ufrj.br, alandes@coc.ufrj.br
[2]*CERIS, DECivil, Instituto Superior Técnico, Universidade de Lisboa*
Av. Rovisco Pais, 1049-001, Lisboa, Portugal
dcamotim@civil.ist.utl.pt

Abstract. This paper reported the results of an ongoing numerical (ABAQUS shell finite element) investigation on the distortional buckling, post-buckling and ultimate strength behaviours and DSM (Direct Strength Design) Design of cold-formed steel beams subjected to major-axis non-uniform bending due to one mid-span point load (transverse applied load). The beams analysed consisted of single-span lipped channel members exhibiting (i) 15 geometries, (ii) end sections that are locally and globally pinned and may warp freely, (iii) triangular bending moment diagrams, and (iv) 8 yield stresses, selected to cover a wide distortional slenderness range. After acquiring in-depth insight into how the triangular bending moment diagram influences the beam distortional buckling and post-buckling behaviours, an extensive numerical (shell finite element) parametric study is carried out in order to gather significant distortional failure moment data concerning lipped channel beams. These failure moments are then employed to assess the merits of the available DSM beam distortional strength curves in predicting them, namely (i) the one currently codified in North America (AISI 2016) and (ii) those proposed by Martins *et al.* (2017). The above curves were found to be inadequate for providing safe and accurate predictions of failure moments, highlighting the need to continue developing an efficient and reliable DSM-based design approach for beams failing in distortional modes under non-uniform bending.

Keywords: Cold-formed steel beams; Lipped channel beams; Distortional post-buckling behaviour/failure; Shell finite element analysis; Direct Strength Method (DSM) design.

1 Introduction

The usage of cold-formed structural members provides several advantages over traditional steel elements, including: (i) optimised section shapes maximize material efficiency, and (ii) significant scope for innovation. However, the combination of high-strength steel grades and very slender cross-sections makes these structural systems highly susceptible to instability phenomena, particularly distortional buckling. This often governs the structural response and collapse of "intermediate members", or those with "intermediate lengths". In the specific case of cold-formed steel beams, a fair amount of research work has been devoted to the development/improvement of DSM-based design methodologies [1-8].

The objective of the present work is to extend the scope of the Depolli *et al.* [7] study by investigating beams subjected to non-uniform major-axis bending (caused by transverse loading), namely their (i) buckling, post-buckling and ultimate strength behaviours and (ii) DSM-based design (*e.g.* [6,9]).

2 Buckling Behaviour

As done in previous studies (*e.g.*, [5-8]), the first task of this work consists of selecting the geometries (cross-section dimensions and lengths) of the single-span CFS lipped channel beams (LCB) with transverse loading to be analysed, as depicted in Fig. 1(a). Using the principle of force transmissibility [12, 13], as shown in Fig. 1(b), the vertical load (P) was converted into a vertical load at the juncture of the web and top flange, and a pair of opposite lateral loads at the junctures of the web with the top and bottom flanges ($Q = P\ d_{SC}/b_w$ – see Fig. 1(b)). These loads (P and Q) are linearly distributed as p and q across the nodes of the beam section: $p = P/(n_y + 1)$ and $q = Q/(n_x + 1)$ and for the web and flanges, where n_y and n_x are the numbers of elements on web and flanges, respectively (see further details in [13]).

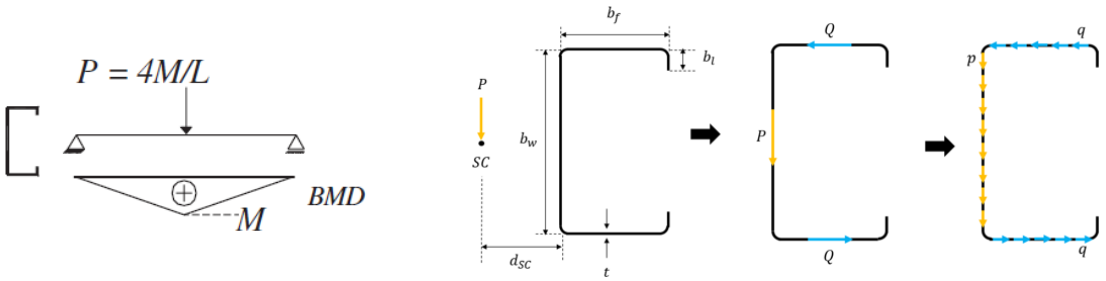

Figure 1. (a) Bending moment diagram considered for the LCB, (b) loading transformation for LCB.

The selection procedure considered initially the beams geometry and lengths previously reported by Depolli *et al.* [7] (for end-moments loading), involving sequences of buckling analyses, performed by means of the code GBTUL [10] (based on Generalized Beam Theory – GBT) or ABAQUS SFEA and intended to identify beams buckling and failing in "pure" distortional modes – *i.e.*, such that their D (critical) buckling moments are well below their local and global bifurcation moments. The output of the above effort is the *15* LCB cross-sections whose dimensions (b_w, b_f, b_l, t – see Fig 1(b)) are given in Table 1, which also displays their area (A) and major-axis elastic (S) and plastic (Z) moduli (note that these beams are the same as those selected in [7]). Moreover, this table also provides (i) the critical distortional buckling lengths (L_D) and moments (M_{crD}), (ii) the ratios M_{crL}/M_{crD} and M_{crG}/M_{crD} (M_{crL} and M_{crD} are the lowest local and global bifurcation moments) – all buckling/bifurcation moments were for *E=210 GPa* and *v=0.3* (typical steel Young's modulus and Poisson's ratio values). It is worth mentioning that (i) the beams selected exhibit single half-wave critical distortional buckling modes and (ii) M_{crL}/M_{crD} and M_{crG}/M_{crD} lie in the ranges *1.42-4.94* and *25.79-182.90*.

Table 1. Cross-section dimensions, properties, critical buckling lengths, moments, buckling moment ratios.

Beam	b_w (mm)	b_f (mm)	b_l (mm)	t (mm)	*Area* (cm²)	S (cm³)	Z (cm³)	L_D (cm)	M_{crD} (kNcm)	$\frac{M_{crL}}{M_{crD}}$	$\frac{M_{crG}}{M_{crD}}$
C01	75	65	5	2	4.3	12.3	13.3	20	289.49	4.68	182.90
C02	90	75	6.25	1.8	4.5	15.5	16.7	30	264.62	3.89	151.54
C03	120	75	10	3	8.7	37.2	41.1	45	1886.18	3.52	25.79
C04	120	80	10	2.5	7.5	32.5	35.8	35	1039.50	3.38	75.17
C05	130	80	10	3	9.3	43.0	47.5	35	1657.78	3.82	62.58
C06	135	75	10	2.7	8.2	38.7	43.0	35	1500.36	3.03	55.73
C07	135	85	10	2.8	9.1	43.9	48.4	35	1424.76	3.52	82.59
C08	140	100	10	2.5	9.0	46.2	50.5	45	933.08	3.50	106.41
C09	150	80	10	2.5	8.3	42.7	47.6	40	1288.40	2.76	61.47
C10	150	100	10	2.5	9.3	50.2	55.1	45	945.63	3.67	114.56
C11	150	120	10	3.5	14.4	80.7	87.6	55	1900.94	4.94	111.57
C12	160	100	10	2.2	8.4	47.7	52.6	45	942.48	2.61	109.73
C13	165	85	10	2.4	8.5	48.1	53.7	40	1189.70	2.42	83.63
C14	225	90	12	2.9	12.4	90.2	102.8	45	2594.70	1.43	65.80
C15	275	110	13	3	15.6	138.3	157.7	55	2897.95	1.42	88.06

For illustrative purposes, the two sets of signature curves M_{cr} vs. L (logarithmic scale) depicted in Fig. 2(a) provide the variation of the elastic critical buckling moment with the beam length C14 beams (see Table 1), considering: (i) uniform bending diagram (for comparison) and (ii) the non-uniform one (see Fig. 1(a)) – the (distortional) critical buckling mode of the selected beam are also provided. The observation of these two sets of plots leads to the following comments:

(i) As expected and also previously observed by Bebiano *et al.* [14], the curve concerning the LCB subjected to non-uniform bending exhibits initial rising branches (somewhat "irregular") within the range $10 < L < 100$ cm (point load). Most of the subsequent descending branches (for $L > 200$ cm) are associated with lateral-torsional buckling. At this stage, it is worth recalling that the reference moment includes the beam length (it is proportional to PL), which means that, although the critical P values decrease monotonically with L, the same does not occur with the corresponding reference moments.

(ii) The uniformly bent beam curve exhibits a number of well-defined local minima, associated with local-plate ($10 < L < 40$cm) and distortional ($40 < L < 200$cm) buckling. For $L > 200$ cm, the beam buckling is lateral-torsional with a bit of distortion.

(iii) Generally speaking, non-uniform bending only leads to reference M_{cr} values higher than the uniform bending ones for $L > 100$cm — the exception is lengths $200 < L < 240$cm.

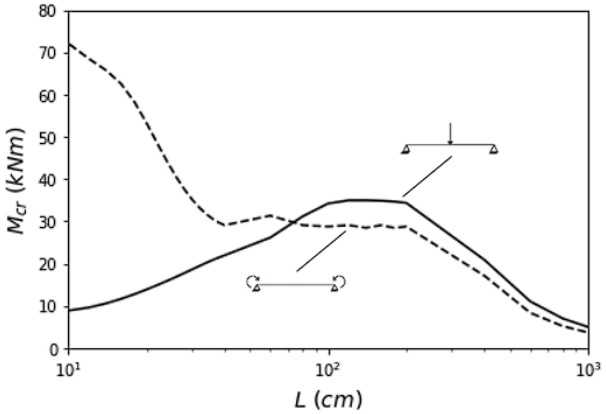

Figure 2. Variation of M_{cr} with L and for C14 LCB subjected to (i) uniform and (ii) non-uniform bending diagram.

3 Distortional Post-Buckling Behaviour

3.1 Numerical model

The beam distortional post-buckling equilibrium paths and ultimate strength values were determined through ABAQUS [11] geometrically and materially non-linear shell finite element analyses (SFEA), employing models similar to those used in previous studies (*e.g.*, [6-8]). The beams were discretised into SHELL elements (*4*-node shear deformable thin-shell elements with six degrees of freedom per node and full integration). The analyses were performed by means of an incremental-iterative technique combining Newton-Raphson's method with an arc-length control strategy. As stated earlier, the beams analysed are simply supported. The bending moment diagram (see Fig. 1(a) is achieved through the application of sets of concentrated forces acting on the nodes of both mid-span cross-sections section p and q (see Fig 1(b)). The force application is made in small increments, taking advantage of the ABAQUS automatic "load stepping procedure". Moreover, all the materially non-linear analyses assumed an elastic-perfectly plastic steel material behaviour following Prandtl-Reuss's plasticity model, which combines von Mises yield criterion with its associated flow rule. All the beams contained initial geometrical imperfections with a critical-mode (distortional) shape and small amplitude (*10%* of the wall thickness t). These initial imperfections involve inward compressed flange-lip motions, since they are known to be the most detrimental, in the sense of leading to lower post-buckling strengths (*e.g.*, [6-8]). Each critical buckling mode shape is obtained by means of a preliminary ABAQUS buckling analysis, performed with exactly the same shell finite element mesh employed to carry out the subsequent non-linear (post-buckling) analysis – this procedure makes it very easy to "transform" the buckling analysis output into a non-linear analysis input. It is still worth noting that no strain-hardening, residual stresses and/or corner strength effects were considered.

3.2 Elastic-Plastic Post-Buckling Behaviour

Attention is now turned to investigating the elastic-plastic post-buckling behaviour of the beams considered in this work (LCB beams buckling and failing in distortional modes when subjected to transversal loads). Moreover, it is also intended to gather fairly considerable failure moment data, which will be subsequently used to assess the adequacy of the currently codified DSM beam distortional design curve in predicting them. The numerical results presented and discussed concern a total of *135* LCB, combining (i) the *15* geometries defined in Table 1 and (ii) *9* yield stresses, which enable covering wide distortional slenderness ranges (λ_D varies between *0.35* and *4.5*). Fig. 3 shows a sample of the elastic and elastic-plastic post-buckling equilibrium paths M/M_{crD} vs. $|\delta|/t$, obtained for LCB C01-C06 – the elastic paths are displayed for comparison purposes. Fig. 4 depicts the deformed configurations and von Mises stress (σ_{VM}) contours, at the peak/failure moments M_u (identified by white circles on the paths of Fig. 3), of the C01 beams with various λ_D – the distortional nature of the beam collapse modes is clearly visible for all λ_D values.

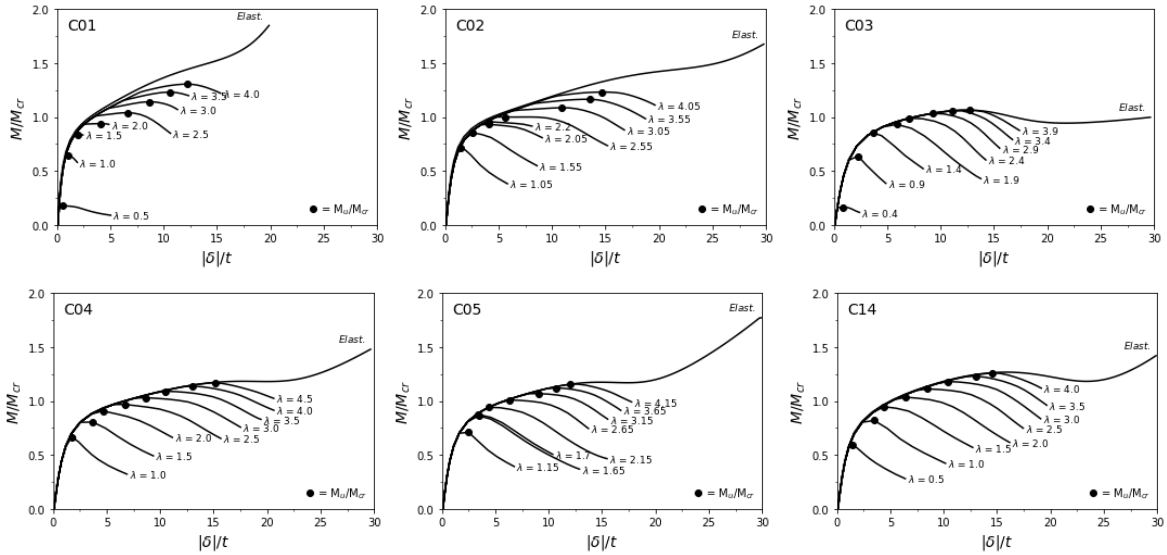

Figure 3. Elastic and elastic-plastic distortional post-buckling equilibrium paths (M/M_{crD} *vs.* $|\delta|/t$), concerning C01-C02-C03-C04-C05-C14 LCB exhibiting various λ_D values.

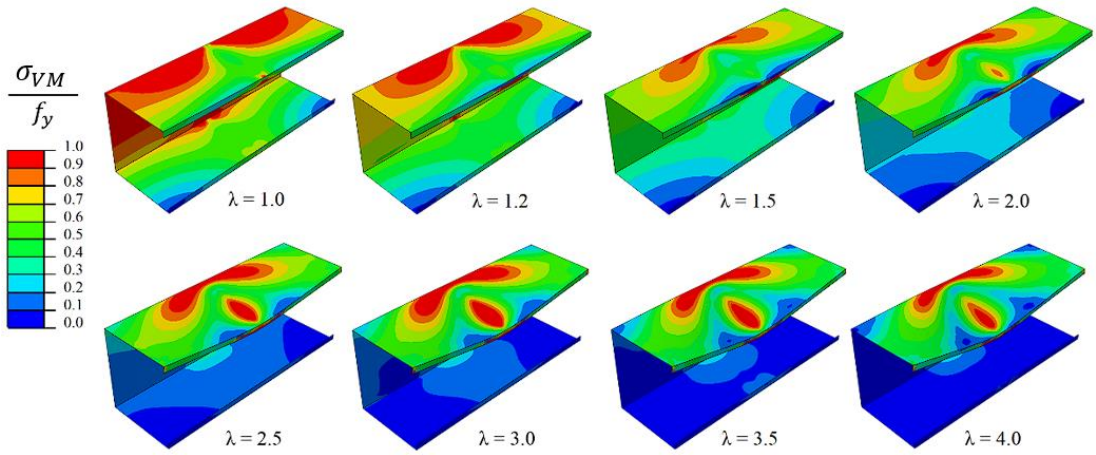

Figure 4. Failure modes and von Mises stress contours concerning C01 LCB exhibiting various λ_D values.

4 Direct Strength Method (DSM) Design Considerations

This section addresses the applicability of the available Direct Strength Method (DSM) distortional design curve to predict the numerical failure moment data concerning the beams considered in this work. For beams with (i) cross-sections symmetric with respect to the bending axis or (ii) cross-sections for which first yield occurs in compressed fibres, the currently codified DSM design curve against beam distortional failures is defined as

$$M_{nD} = \begin{cases} M_y + (1 - C_{yd}^{-2})\left(M_p - M_y\right) & \lambda_D \leq 0.673 \\ \left(1 - 0.22\lambda_D^{-1}\right)\lambda_D^{-1} M_y & \lambda_D > 0.673 \end{cases} \quad , \quad (1)$$

where M_{nD} is the beam distortional nominal strength, M_y and M_p are the beam yield and plastic moments, respectively, $\lambda_D=(M_y/M_{crD})^{0.5}$ is the beam distortional slenderness and $C_{yd}=(0.673/\lambda_D)^{0.5}\leq 3$. On the other hand, Martins *et al.* [6] very recently proposed, in the context of cold-formed steel beams subjected to uniform bending, two novel DSM-based distortional design/strength curves – warping and local displacements/rotations completely free and fully prevented, respectively. They can be cast in the general form

$$M_{nD}^{*} = \begin{cases} M_y + (1 - C_{yd}^{-2})\left(M_p - M_y\right) & \lambda_D \leq 0.673 \\ \left(1 - a\lambda_D^{-b}\right)\lambda_D^{-c} M_y & \lambda_D > 0.673 \end{cases} \quad , \quad (2)$$

where the values of parameters *a*, *b* and *c* are equal to *0.25*, *1.75* and *1.75*, for simply supported LCB.

Figure 5 compares the available DSM distortional design curves (Eqs. (1) and (2)) with the numerical M_u/M_y values obtained in this work. Moreover, Figs 6(a)-(b) plot the numerical-to-predicted failure moment ratios M_u/M_{nD} and M_u/M_{nD*} against the distortional slenderness λ_D, thus providing pictorial assessments of the safety and accuracy of the distortional failure moment estimates yielded by the available strength curves – their statistical indicators (averages, standard deviations, maximum/minimum values – the numbers of "visibly unsafe" failure moment predictions, in the sense that $M_u/M_{nD} < 0.95$ or $M_u/M_{nD*} < 0.95$, are also provided. The observation of the results prompts the following remarks:

(i) In all the plots displayed in Fig. 5, the overwhelming majority of M_u/M_y values are fairly well aligned along a "Winter-type" curve with a small scatter (vertical dispersion).

(ii) The failure moments obtained in this work, for the LCB with transverse loading, are poorly (accurately and safely) predicted by the currently codified DSM design curve in the all-considered slenderness range. Note that the amount of underestimation tends to grow with λ_D and is particularly severe for the slenderest LCB.

(iii) Figures 6(a)-(b) clearly show the failure moment prediction quality improvement achieved by the strength curves proposed by Martins *et al.* [6], spanning the whole distortional slenderness range (even if they were developed solely in the context of uniformly bent beams). The M_u/M_{nD*} statistical indicators are significantly better than their M_u/M_{nD} counterparts. Nevertheless, it must be recognised that there are still fairly high numbers of "visibly unsafe" failure moment predictions ($M_u/M_{nD*} < 0.95$).

To enhance the accuracy of predicting failure moments for beams under transverse loading, a new or modified strength curve should be proposed. The curve reported by Martins *et al.* [1] serves as a good starting point for this task. The authors are actively working on this research, and the results will be shared in the near future.

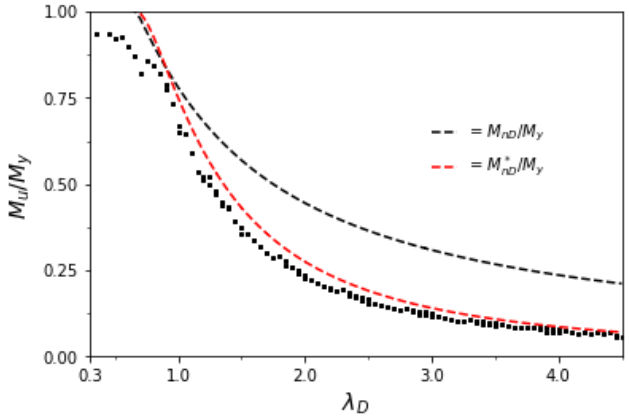

Figure 5. Comparison between the LCB failure moment ratios M_u/M_y obtained in this work with the available DSM distortional strength curves.

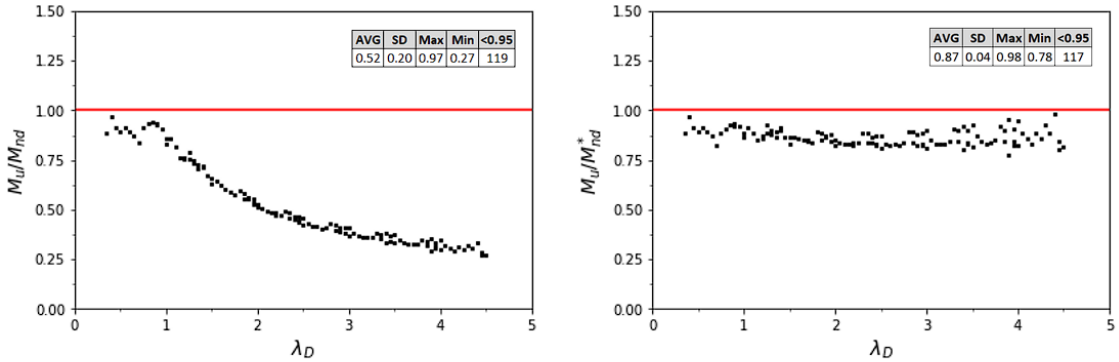

Figure 6. Plots (a) M_u/M_{nD} vs. λ_D and (b) M_u/M_{nD*} vs. λ_D for the LCB considered in this work.

5 Conclusions

This paper reported the most recent results of an investigation, initiated a few years ago [5-8], on the post-buckling behaviour, ultimate strength and DSM design of cold-formed steel single-span simply supported lipped channel beams buckling in distortional modes. After addressing the beam geometry selection and the influence of the temperature on the beam distortional post-buckling behaviour, numerical failure moment data were obtained for 135 beams (see Section 4). The numerical distortional failure moments obtained in this work were subsequently used to assess the merits of the available DSM beam distortional strength curves in predicting. It was found that the above prediction quality is (i) poor for the codified design curve (as expected) and (ii) still inadequate for the design curves developed by Martins *et al.* [6]. Therefore, it is still necessary to search for new design curves providing efficient (safe and reliable) failure moment predictions.

Acknowledgements. The first two authors gratefully acknowledge the financial support of the Brazilian institutions (i) CAPES (Coordenação de Aperfeiçoamento de Pessoal de Nível Superior) – Finance Code 001 (both authors), (ii) CNPq (Conselho Nacional de Desenvolvimento Científico e Tecnológico) – Finance Code 313197/2020-2 (second author) and (iii) FAPERJ (Fundação Carlos Chagas Filho de Amparo à Pesquisa do Estado do Rio de Janeiro) – Finance Code E-26/200.959/2021 (second author). The third author gratefully acknowledges the financial support of FCT (Fundação para a Ciência e a Tecnologia – Portugal) – project UIDB/04625/2020 (funding the research unit CERIS).

Authorship statement. The authors hereby confirm that they are the sole liable persons responsible for the authorship of this work, and that all material that has been herein included as part of the present paper is either the property (and authorship) of the authors, or has the permission of the owners to be included here.

References

[1] Yu C, Schafer BW (2007). Simulation of cold-formed steel beams in local and distortional buckling with applications to the Direct Strength Method, *Journal of Constructional Steel Research*, **63**(5), 581-590.

[2] Bebiano R, Dinis PB, Silvestre N, Camotim D (2007). On the application of the Direct Strength Method to cold-formed steel beams subjected to non-uniform bending, *Proceedings of 5th International Conference on Advances in Steel Structures* (ICASS 2007 – Singapore 5-7/12), J.Y.R. Liew, Y.S. Choo (eds.), Research Publishing (Singapore), 322-327 (vol. III).

[3] Dinis PB, Camotim D (2010). Local/distortional mode interaction in cold-formed steel lipped channel beams, *Thin-Walled Structures*, **48**(10-11), 771-785.

[4] Wang L, Young B (2014). Design of cold-formed steel channel with stiffened webs subjected to bending, *Thin-Walled Structures*, **85**(December), 81-92.

[5] Landesmann A, Camotim D (2016). Distortional failure and DSM design of cold-formed steel lipped channel beams under elevated temperatures, *Thin-Walled Structures*, **98A**(January), 75-93.

[6] Martins AD, Landesmann A, Camotim D, Dinis PB (2017). Distortional failure of cold-formed steel beams under uniform bending: behaviour, strength and DSM design, *Thin-Walled Structures*, **118**(September), 196-213.

[7] Depolli I, Landesmann A, Camotim D, Martins AD (2018). Distortional Failure and DSM Design of Cold-Formed Steel Lipped Channel Beams under Non-Uniform Bending, *Website Proceedings of Structural Stability Research Council (SSRC) 2018 Annual Stability Conference*, Baltimore, 10-13 de Abril, 2018.

[8] Neves NS, Landesmann A, Camotim D (2024). CFS lipped channel beams buckling in distortional modes at elevated temperatures: Behaviour, failure and DSM design, *Thin-Walled Structures*, **195**(February), 111366

[9] AISI (American Iron and Steel Institute) (2022). *North American Specification (NAS) for the Design of Cold-Formed Steel Structural Members* (2016 edition reaffirmed in 2020 with Supplement 3), AISI-S100-16 w/S3-22, Washington DC.

[10] Bebiano R, Camotim D, Gonçalves R (2018). GBTUL 2.0 – a second-generation code for the GBT-based buckling and vibration analysis of thin-walled members, *Thin-Walled Structures*, **124**(March), 235-257.

[11] Simulia Inc. (2014). ABAQUS Standard (version 6.14-1).

[12] Wan H-X, Huang B, Mahendran M (2021). Experiments and numerical modelling of cold-formed steel beams under bending and torsion, *Thin-Walled Structures*, **161**(April), 107424.

[13] Xia Y, Glauz RS, Schafer BW, Seek M, Blum HB (2024). Cold-formed steel strength predictions for torsion and bending–torsion interaction, *Thin-Walled Structures*, **195**(February), 111367.

[14] Bebiano R, Silvestre N, Camotim D (2007). GBT formulation to analyze the buckling behavior of thin-walled members subjected to non-uniform bending, *International Journal of Structural Stability and Dynamics*, **7**(1), 23-54.